International Journal of Hyperthermia

ISSN: 0265-6736 (Print) 1464-5157 (Online) Journal homepage: www.tandfonline.com/journals/ihyt20

Ultrasound-guided therapeutic focused ultrasound: Current status and future directions

Emad S. Ebbini & Gail Ter Haar

To cite this article: Emad S. Ebbini & Gail Ter Haar (2015) Ultrasound-guided therapeutic focused ultrasound: Current status and future directions, International Journal of Hyperthermia, 31:2, 77-89, DOI: 10.3109/02656736.2014.995238

To link to this article: https://doi.org/10.3109/02656736.2014.995238

Published online: 23 Jan 2015.

International Journal of Hyperthermia

http://informahealthcare.com/hth
ISSN: 0265-6736 (print), 1464-5157 (electronic)

Int J Hyperthermia, 2015; 31(2): 77–89
 DOI: 10.3109/02656736.2014.995238

informa healthcare

REVIEW ARTICLE

Ultrasound-guided therapeutic focused ultrasound: Current status and future directions

Emad S. Ebbini[1] & Gail Ter Haar[2]

[1]Electrical and Computer Engineering, University of Minnesota Twin Cities, Minneapolis, Minnesota, USA and [2]Joint Department of Physics, Division of Radiotherapy and Imaging, Institute of Cancer Research, London, UK

Abstract

This paper reviews ultrasound imaging methods for the guidance of therapeutic focused ultrasound (USgFUS), with emphasis on real-time preclinical methods. Guidance is interpreted in the broadest sense to include pretreatment planning, siting of the FUS focus, real-time monitoring of FUS-tissue interactions, and real-time control of exposure and damage assessment. The paper begins with an overview and brief historical background of the early methods used for monitoring FUS-tissue interactions. Current imaging methods are described, and discussed in terms of sensitivity and specificity of the localisation of the FUS effects in both therapeutic and sub-therapeutic modes. Thermal and non-thermal effects are considered. These include cavitation-enhanced heating, tissue water boiling and cavitation. Where appropriate, USgFUS methods are compared with similar methods implemented using other guidance modalities, e.g. magnetic resonance imaging. Conclusions are drawn regarding the clinical potential of the various guidance methods, and the feasibility and current status of real-time implementation.

Keywords

Boiling histotripsy, cavitation, FUS-mediated drug delivery, high intensity focused ultrasound, thermal therapy

History

Received 13 October 2014
Revised 1 December 2014
Accepted 2 December 2014
Published online 23 January 2015

Introduction

The therapeutic potential of focused ultrasound (FUS) as a means of localised destruction of deep tissue structures has been known for decades, having first been demonstrated *in vivo* in the 1950s [1–5]. At high intensities, in the range 10^2–10^4 W/cm^2, high intensity focused ultrasound (HIFU) has been known to produce a range of therapeutic and sub-therapeutic effects, depending on the exposure duration. For example, at intensity levels of the order of 10^3 W/cm^2 and exposure durations of the order of 1 s, HIFU produces thermal coagulation within the small volumes determined by the size of the focal spot. HIFU is a widely, but imprecisely, used acronym. In this paper FUS is used to refer to focused ultrasound regardless of the focal intensity. HIFU is used to describe exposures producing thermal or non-thermal irreversible change within seconds. Several research groups have investigated the thresholds for lesion formation and established dose response formulae on theoretical and empirical grounds [6–8]. Results from these studies have led to identification of two distinct regions of tissue damage that can be attributed to thermal and cavitational mechanisms, respectively. Thermal damage is associated with relatively 'low' intensities of $\sim 10^2$ W/cm^2, and exposure times of $\sim$1–10 s. Cavitation-mediated damage is associated with peak intensities above 2000 W/cm^2 and exposure times shorter than 40 ms. Data from three different laboratories from studies of thresholds for lesion formation in the white matter of the mammalian brain are in good agreement for exposure durations in the range of 0.05–10 s [8]. A threshold dose relationship of the form $I\sqrt{t} = C$ was proposed for tissue ablation by Frizzell [6], where I is the spatial peak of the delivered intensity and t is the exposure duration. This formula was shown to be applicable to exposure durations in the 0.1–10-s range in the brain ($C = 200$ W/cm^2 s$^{0.5}$) and liver ($C = 460$ W/cm^2 s$^{0.5}$). The exposure time range agrees well with the thermal dose concept of Sapareto and Dewey [9,10], thus strongly supporting the thermal damage hypothesis. Shorter exposure durations at higher peak intensities caused non-thermal damage due to cavitation.

Tissue damage by cavitation was not well understood in these early studies, but it was clear that short exposures (<0.05 s) and intensities above 2500 W/cm^2 resulted in 'cavitation lesions' [8]. Studies by Fry and co-workers [8], based on their own experimental work, and incorporating published results from other laboratories, concluded that three types of FUS-induced lesions were formed in mammalian white matter: (1) low intensities and long exposure duration resulted in thermally induced lesions, (2) higher intensities and short exposure durations resulted in cavitation induced

Correspondence: Emad Ebbini, 200 Union Street SE, Minneapolis, MN 55455, USA. Tel: +1(612) 625 - 1852. Fax: +1(612) 625 - 4583. E-mail: emad@umn.edu

lesions, and (3) intermediate exposures (both in intensity and exposure time) resulted in mechanically induced lesions, but the mechanism for these was not well understood, since cavitation activity was not monitored [8].

Until recently, the thermotherapy applications of FUS have been dominant, probably due to the incomplete understanding of cavitational and mechanical effects. Interest in ultrasound hyperthermia gained some momentum in the 1980s and early 1990s [11–20]. An excellent review of the status of FUS hyperthermia in the early 1980s can be found by Lele [21]. Rapid heating hyperthermia [22] gained some interest in the early 1990s as a way of countering the effects of blood perfusion. For both conventional and rapid heating hyperthermia, it was emphasised that FUS intensities below the threshold for transient cavitation should be used [7,21]. By the late 1990s, research and development activity was mainly focused on high-temperature (ablative) applications, and some viable commercial ultrasound-guided HIFU systems appeared. It was clear that cavitation played a role in lesion formation when moderately high intensity levels were used, even though the lesions generally exhibited the characteristics of thermal damage. This led to a number of investigations designed to elucidate the positive role played by cavitation in thermal lesion formation [23]. New non-thermal therapies, based on the use of intense, low duty cycle FUS exposures, e.g. histotripsy [24–28] and boiling histotripsy [29] have been introduced. This wide spectrum of applications employing the full range of thermal and non-thermal HIFU–tissue interactions emphasises the need for imaging guidance in non-invasive surgical applications.

The advent of non-ionising, real-time diagnostic imaging, together with improved transducer technologies, has encouraged numerous research groups to investigate a variety of therapeutic applications of FUS, especially as a stand-alone, minimally invasive method for cancer therapy [30–33], thrombolysis [34] and haemostasis [35] among others. These new applications increasingly employ cavitational mechanisms, with and without the use of microbubble ultrasound contrast agents (UCA). The wide range of applications and the use of both thermal and non-thermal bioeffects of FUS have heightened the need for new imaging methods for guidance. Not only do we need anatomical imaging for visualisation of the target and placement of the FUS beam, but we also need imaging methods with higher sensitivity and specificity to FUS–tissue interactions in both therapeutic and sub-therapeutic modes.

Ultrasound guidance for visualisation of target tissue was proposed by Fry and others in the early days of diagnostic ultrasound (in the 1970s), and continued to be the only guidance modality until the early 1990s [36–38]. By the mid to late 1990s however, magnetic resonance (MR) guidance of FUS treatments had been demonstrated by Hynynen and colleagues [39,40], and later by other groups [31,41–43]. These two modalities continue to be the leading image guidance techniques for both clinical and preclinical therapeutic FUS systems. The two methods have enabled, and helped to demonstrate, the potential of FUS in a number of clinical applications, underwriting the adoption of FUS for newer clinical applications, including transcranial focusing [44]. In addition to standard diagnostic imaging, specialised modes suitable for the guidance of thermal and non-thermal FUS procedures have also been developed and implemented in real time, e.g. MR and ultrasound thermography [45–53] and elastography [33,43,54–59].

In the following, we review the current status and future directions of ultrasound-guided FUS (USgFUS) systems. Methods with high specificity to FUS–tissue interactions are emphasised and will be described in some detail here. We also address their applicability to planning, targeting, monitoring, control, and assessment of the therapeutic procedure. The feasibility of *in vivo* real-time implementation for each method is also discussed.

FUS–tissue interactions and implications for image guidance

Thermal effects

Ultrasound-induced temperature rise is dependent on the local exposure conditions (e.g. intensity, duration and duty cycle) and local tissue properties (e.g. absorption coefficient, perfusion). For longer exposure durations the beam geometry and scanning configuration play an important role. Despite obvious limitations, the Pennes' transient bioheat equation has been shown to provide an adequate model for temperature evolution [60]. The thermal effects of ultrasound arising from absorption mechanisms are described using linear and non-linear propagation models of FUS beams [11,61–63]. It is well known that both stable and transient cavitation contribute to the observed temperature change, although it is challenging to model these effects [64]. From the image-guidance perspective, however, the localised nature of the thermal effects defines the requirements for the different guidance methods. The relatively short wavelength of ultrasound in the MHz frequency range, together with focusing give FUS a unique advantage as a means of minimally invasive surgery [11,21]. A typical FUS transducer concentrates the bulk of a beam's energy within focal volumes of the order of $1\lambda \times 1\lambda \times K\lambda$, where λ is the wavelength, and K is a constant determined by the transducer geometry (typical values are 5–7). This allows tailored, localised heating of targets near critical structures (such as bone or major vessels) with minimal or no collateral damage. The key to thermal therapy using FUS is the local absorption of energy within the focal volume. This may be orders of magnitude greater than in the intervening and surrounding tissue, especially when non-linear effects are taken into account [63]. With a proper treatment plan based on acoustic and thermal properties of the target volume it is possible to design a FUS field pattern (using a shell, lens-focused or phased array transducer) which provides high heating rates within the focal spot while minimising the heating rate in the skin, mucosa, and subcutaneous tissues.

Tight focusing allows the intensity to decay rapidly in tissues beyond the focus, due to beam divergence and attenuation. This makes it possible to place the focal region very close to critical structures lying beyond the target volume, such as bone, without excessive collateral damage. Tight focusing is also advantageous when heating near thermally significant blood vessels. In these cases, FUS beams can be used to produce highly localised thermal coagulation of tissues very close to the vessel wall, leaving endothelial cells intact

[65]. Incomplete coagulation near thermally significant blood vessels presents a challenge to methods such as RF ablation [66,67]. Clearly, the small size of the focal region is disadvantageous when large tissue volumes are to be ablated, but phasing and motion strategies may be applied to enlarge regions treated during single exposures [68,69].

The potential of FUS as a precise, non-invasive form of surgery can clearly only be realised when advanced image guidance is used as the enabling technology for, at a minimum, target visualisation and beam siting within the treatment zone. More importantly, however, the full potential is only achievable if there is high specificity to monitoring FUS-tissue interactions. In the context of thermal therapy, non-invasive imaging of temperature (change) is of significant, if not critical, value for the monitoring and control of the FUS application. To the extent that bubbles play a relevant role in lesion formation (e.g. in bubble-enhanced heating), imaging and localisation of bubble activity would also be very important in monitoring and post-treatment evaluation. It is also known that the tissue's elastic properties change upon thermal coagulation, which suggests the use of elastography for damage assessment within the treatment zone.

Mechanical effects

Cavitation can occur *in vivo* if appropriate microbubbles are present, for example as contrast agents or in tissue gas inclusions (as found in the intestine). Bubble oscillations under the influence of an acoustic field are characterised as non-inertial (stable) or inertial (collapse). Lele [70] argues correctly that non-inertial cavitation has no distinct pressure threshold for its initiation. On the other hand, inertial cavitation is a threshold phenomenon. Its threshold depends on the tissue type, frequency, baseline temperature, ambient and acoustic pressures (peak-positive and peak-negative), and pulse repetition frequency (PRF). A combination of the PRF and pulse properties such as peak-positive and peak-negative pressures can be used in creating and maintaining bubble clouds that in turn produce significant mechanical effects on tissue, such as tissue erosion in histotripsy [71]. Boiling histotripsy is another method used for homogenisation of the tissue within the lesion, with or without using the thermal effects of HIFU [29].

Another mechanical effect of pulsed FUS (pFUS or pHIFU) is related to the acoustic radiation force (ARF). The ARF results from the transfer of momentum from the sound field to an object. This transfer of momentum occurs at reflecting surfaces or within absorbing propagation media. This effect is the basis of several elasticity imaging methods, such as ARF imaging (ARFI) [72,73] and shear wave elasticity imaging [74–77]. It is also believed to be the basis of some therapeutic applications such as bone healing and cardiac pacing, probably in combination with cavitation [78,79].

The monitoring of cavitation-mediated therapeutic procedures has been achieved by passive cavitation detection, in which a broadband hydrophone is focused on the FUS target volume [23,70]. Most recently, however, array beamforming of the emission has allowed detection, and the mapping of cavitation activity has been made possible [80]. Stable cavitation bubbles linger for seconds after their nucleation by FUS and can be actively imaged and localised using linear and non-linear methods [81–83] or ultrafast active imaging [84]. The radiation force effect can be readily imaged using methods which employ speckle tracking for elastography and thermography, in conjunction with high frame-rate imaging [77,85].

Agent-mediated FUS–tissue interactions

Only brief coverage is given in this section of this vast topic in which an agent is used to enhance the therapeutic effects of FUS beams. This can be achieved, for example, by lowering the threshold for cavitation or enhancing local absorption. A closely related topic is the delivery and/or release of therapeutic agents using FUS [86,87]. The use of microbubble UCA has been proposed either for enhancing, or assessing, the efficacy of some FUS procedures [88–91]. These include drug [86] and gene delivery [91,92] and opening of the blood–brain barrier [93]. Standard UCA imaging methods can be used to characterise microbubble activity, and to provide correlation with the therapeutic end point.

Acoustic droplet vaporisation (ADV) has also been suggested for the enhancement of some FUS procedures [94,95]. This method converts biocompatible micro- or nanodroplets into microbubbles that in turn locally enhance effects induced by HIFU. These may have a unique advantage over UCA microbubbles, which may interact with the ultrasound beam both within, and outside, the focal volume, thus potentially causing collateral damage. Once in microbubble form (after appropriate HIFU exposure), detection and localisation of ADVs can be accomplished using one of the passive or active cavitation detection methods mentioned above.

Real-time USgFUS methods *in vivo*

In this section we give appropriate examples of USgFUS methods from the literature. Real-time imaging is interpreted loosely here, referring to real-time data acquisition, although the algorithm may be implemented offline. We emphasise implementations here that have been demonstrated *in vivo*, but some examples based on *in vitro* or *ex vivo* experiments when the set-up and implementation are clearly applicable *in vivo* are also included. This section addresses the different aspects of USgFUS for therapeutic applications: pretreatment planning, beam siting, monitoring, control, and assessment.

Pretreatment planning

Traditionally, pretreatment planning of hyperthermia and other FUS procedures has been based on acoustic and thermal simulations with different levels of heterogeneity [20,68,69,96–102]. For more challenging targets, as in transcranial focusing, the simulation model has typically been derived from 3D MR or CT patient data sets [103–105]. More recently, USgFUS methods for refocusing based on pretreatment ultrasound imaging data have been proposed. An image-based algorithm for refocusing an array in the presence of strongly scattering targets (e.g. the ribs) has been presented [106]. In this case, ultrasound images of the target region, which include Plexiglas rods to simulate the ribs, were acquired in order to define the target focus point(s) and the rib locations in the path of the HIFU beam. Experimental

validation of algorithm(s) described by other authors [106–110] has also shown that the focusing gain at the target can be improved while minimising the exposure to ribs.

The modelling and optimisation of HIFU treatments of peripheral vessels using diagnostic ultrasound has been suggested [111]. In the study described by Shehata et al. [65], diagnostic ultrasound images showed the target vessel and plaque burden as well as the anatomical structure of the target volume. A manual segmentation algorithm was used to identify the tissue types, based on the known anatomy. The result of this segmentation was then used as the input to a heterogeneous acoustic and temperature model used for computation of the temperature evolution and thermal dose accumulation [9] which would result from a prescribed HIFU treatment protocol.

Figure 1 shows a diagnostic B-mode image of the femoral artery of a familial hypercholesterolaemic (FH) pig used in the study described by Shehata et al. [65]. Manual segmentation was used to identify the skin (S), fat (F), muscle (M), and connective tissues (CT) in addition to the artery (A). Tabulated values of the acoustic and thermal properties of these tissues were used to model the lesion formation process during a planned HIFU exposure. Care was taken to acquire the diagnostic ultrasound scan with a level of tissue compression consistent with the compression produced by the therapeutic HIFU transducer. This was achieved by: (1) applying sufficient compression to obtain the best possible diagnostic image, and (2) gradually reducing the compression to the minimum that maintained contact with the skin. This was necessitated by the use of a water bolus to provide coupling with the concave HIFU array. This minimised tissue compression during the treatment.

Identification and positioning of the FUS focus

The dimensions of HIFU beams are in the order of one wavelength in the lateral dimension and a few wavelengths in the axial direction (e.g. from a 1.5 MHz array with low f-number – defined as the ratio of the focal distance and the aperture size in a given direction; the smaller this number, the higher the degree of focusing). In some applications which require high precision, a shifting of the focal location could result in unintended collateral damage to nearby critical structures. Being able to place the FUS focal spot at the desired target location before administering the damaging HIFU 'shot' (using a sub-therapeutic intensity level) would be a highly desirable feature of any USgFUS system.

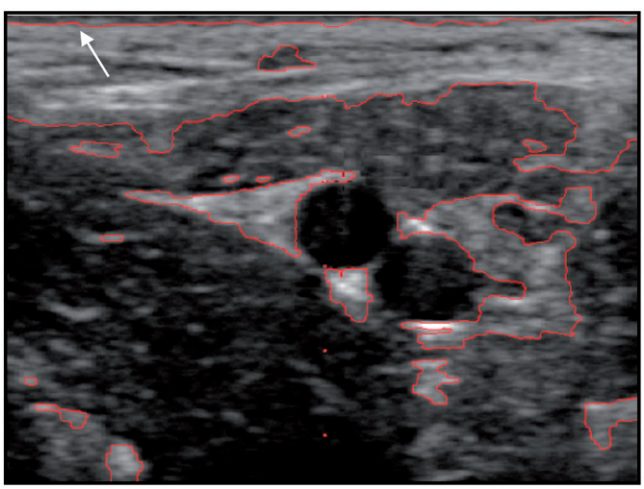

Figure 1. Diagnostic ultrasound image of the target vessel and surrounding tissue used for the determination of the treatment planning model parameters. The target vessel was the femoral artery of a FH pig used in the study described in Shehata et al. [65]. Reproduced with permission from Almekkawy [111]. S, skin; F, fat; M, muscle; CT, connective tissue; A, artery.

Ultrasound backscatter temperature imaging has been proposed for treatment planning of HIFU 'shots' in this fashion [85,112,113]. Imaging of small, localised temperature changes produced by sub-therapeutic FUS beams with sub-second durations allows the estimation of the therapeutic exposure necessary to produce a lesion at that same location. The repeatability of these measurements has been demonstrated e*x vivo* in tissue (porcine heart and liver) [85,112]. *In vivo* experiments have demonstrated the feasibility of compensating for the effects of tissue motion and deformation in a rodent model [114].

Siting of FUS beams using sub-therapeutic intensity levels has been demonstrated using high resolution ultrasound thermography (UST) [112–114] and/or magnetic resonance acoustic radiation force impulse (MR-ARFI) imaging [43,115]. To our knowledge, US elasticity techniques such as ARFI or shear wave elasticity imaging (SWEI) [116], have not as yet been used for siting HIFU beams with sub-therapeutic exposures. This is not due to a fundamental limitation on these methods, and it is quite likely these will be demonstrated in the near future. At present, however, real-time UST has been shown to localise sub-therapeutic HIFU beams both *ex vivo* [48,85] and *in vivo* [114]. A diagnostic ultrasound probe has been used to image a cross section of the sub-therapeutic FUS beam at frame rates at 100 fps or higher [85]. A typical application of sub-therapeutic FUS 'shots' uses intensities in the 100–200 W/cm^2 range, with exposure durations of 0.2–1.0 s. The idea is to produce a small, but measurable, temperature rise above the baseline variation due to natural tissue motion for the *in vivo* case (e.g. as described in [114]).

The relatively high frame-rate imaging employed for real-time imaging of short, localised sub-therapeutic exposures is a clear advantage for USgFUS. At 100 fps or higher, ultrasound speckle tracking has been shown to capture a variety of tissue motions and deformations in anaesthetised small animals (e.g. rats [114]). For example, depending on the depth of anaesthesia, the animal gasps at a quasi-periodic rate of one gasp every 2 s or so. At low frame rates, the co-occurrence of the gasp and the heating FUS 'shot' results in significant shifts that may cause speckle tracking to fail. This, in turn, results in a loss of temperature change tracking. A spatial adaptive filter has been used to remove the contribution of these gasps (and other tissue motions and deformations) from the observed temperature change [114]. This approach has produced an improved localisation of the FUS spot and a better estimation of the initial heating rates at the target location.

Real-time monitoring of FUS-tissue interactions

In principle, therapeutic HIFU applications are based on the sequential adjacent placing of individual 'shots' to produce a

volumetric lesion of specified dimensions. Thermal and non-thermal HIFU techniques differ in the peak intensity (or pressure), pulse duration, and duty cycle used, but the total time per 'shot' is on the order of 0.2–10 s in most applications. Monitoring tissue response during this time with sufficient spatial and temporal resolution would be highly beneficial for treatment control and post-treatment evaluation of actual exposure. An USgFUS method, if proven reliable, would have a unique advantage over other guidance modalities because of the availability of high frame-rate imaging of thermal and mechanical effects [84,85].

The monitoring aspect of USgFUS has been a major emphasis of most active research groups [80,85,117–123]. In addition to the obvious use of hyperechoic changes in standard B-mode imaging, methods for monitoring based on temperature change, radiation force, and cavitation detection and mapping have been demonstrated. A detailed description of each of these contributions would be overly long here. Instead, we give a general description of the methods by category, based on the monitored bioeffect.

Real-time monitoring based on echogenicity change

Increased echogenicity from the location of lesion formation has been observed using real-time sonography since the early days of diagnostic ultrasound [124]. These changes result from individual HIFU 'shots' capable of producing significant bubble clouds, or from tissue water boiling, which results in a significant increase in backscatter [125]. This is the simplest form of monitoring/damage assessment and is currently implemented on some clinical systems [126,127]. This approach provides an indication of tissue response consistent with lesion formation associated with tissue water boiling and vaporisation [128].

A typical configuration of an integrated USgFUS system is shown in Figure 2. A broadband, wide-sector vaginal probe is used in conjunction with a single-element HIFU transducer with the two transducers 'locked' together such that the HIFU focus is within the imaging slice of the imaging transducer. The HIFU exposure is synchronised with the imaging sequence to allow the acquisition of the echoes from the treatment region when the HIFU transducer is 'silent'.

It is now well known that changes in echogenicity cannot be used for localisation due to their lack of spatial sensitivity, especially in standard B-mode. Vaezy et al. [125] investigated the dynamics of echogenicity change and reported high levels of variability of lesion sizes for 'over-exposure' conditions. In addition, the area of the hyperechoic spot on B-mode typically overestimates the actual lesion size, as seen on gross histology. Non-linear imaging methods such as pulse inversion imaging [83] and quadratic imaging based on second-order Volterra filters have been shown to provide more accurate spatial mapping to the actual lesion location on gross histology *ex vivo* [129]. The main limitation of this method, however, is that the lack of significant changes in echogenicity is not necessarily indicative of the failure of HIFU to form a lesion, as ablation may occur in the absence of significant bubble formation. For thermal treatments, while the appearance of hyperechogenicity guarantees tissue ablation, the exposure levels used are thought to be significantly greater than the threshold needed to produce tissue necrosis. In this sense, the tissue has been 'overtreated'.

Real-time monitoring of thermal effects

The temperature rise due to absorption of FUS beams at both therapeutic and sub-therapeutic levels can be monitored by methods such as UST [47,48,112] and change in backscatter energy (CBE) [49,130]. These methods work reasonably well for low to moderate changes in temperature, but tend to fail at high temperatures, for which there is significant decorrelation in the echo data from the focus location. These decorrelations have been exploited as a means of lesion detection during ablative HIFU procedures [112,125,131,132]. High frame-rate imaging demonstrates that the decorrelation is due to transient events consistent with vaporisation of liquid, and the exsolution of formerly dissolved permanent gas out of the liquid and into gas spaces [82,128]. These transients are distinctly different from cavitation effects, but it is quite likely that they coexist with cavitation. Regardless, the detection of these transients can be a reliable indicator of thermal lesion formation for exposure durations longer than 100 ms for most tissues.

Real-time monitoring of cavitation

Traditionally, passive cavitation detection has been used to characterise cavitation activity at the HIFU focus [7,70,133]. Focused passive cavitation detectors (PCDs) for which the focal regions of the HIFU and the PCD transducers overlap are used. The overlap may be coaxial, or at an angle that intercepts the focal region. The spectral power density of the acoustic emission signals picked up by the PCD allows the detection and characterisation of cavitation activity; discrete harmonics and sub-harmonics indicate stable cavitation, while broadband spectra indicate non-inertial or collapse cavitation. These signatures are quite reliable indicators of cavitation and can easily be distinguished from other non-linear phenomena.

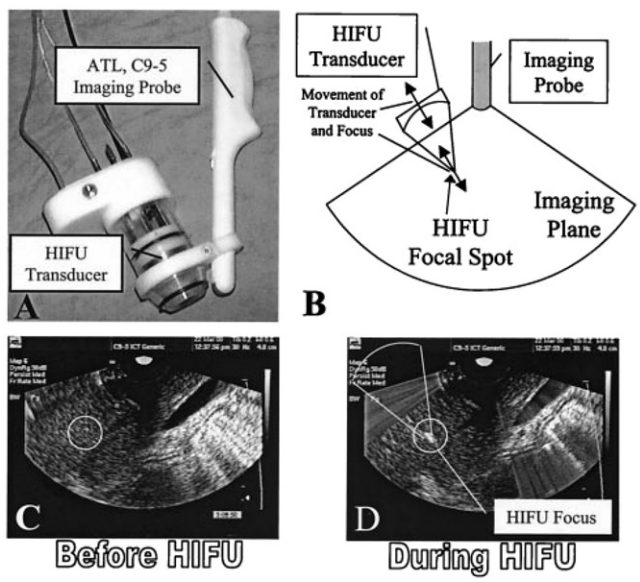

Figure 2. An integrated USgFUS system for real-time visualisation of lesion formation based on echogenicity change. Reproduced from Vaezy et al. [125]. Reproduced with permission from IEEE and Elsevier Science and Technology Journals.

More recently, however, the use of transducer arrays for passive cavitation detection has allowed the use of beamforming methods to map the cavitation activity to its source region (e.g. at the HIFU focus) [134,135].

Real-time control of FUS patterns

Tissue targets are often modified by a HIFU exposure within milliseconds of its start. For example, stable microbubbles are generated almost instantaneously, and it is hypothesised that they grow to a resonant size through rectified diffusion [70]. In this form they may contribute to an increase in the local absorption, but otherwise have minimum effect on delivery of the therapeutic dose. Above certain intensity and exposure thresholds, inertial cavitation or tissue boiling occurs. These can have drastic effects on the resulting lesion size and shape. More significantly, they may affect nearby HIFU 'shot' locations. These effects have been described by many authors based on empirical evidence [7,8,70,136], and there have been efforts to model the lesion formation dynamics with and without accounting for bubble formation [61,62,64]. However, accounting for the dynamics of transient cavitation under the effects of HIFU *in vivo* remains a daunting task. Until recently, open-loop control of thermal lesion formation relied on some form of treatment planning to decide on appropriate values of I and T which give a desirable lesion size and shape. A sufficient waiting time between 'shots' has been used to avoid overexposure due to heat build-up from the individual 'shots' needed to cover the specified target volume (e.g. the whole prostate in transrectal HIFU treatment). This build up may be focal or pre-focal. This prolonged treatment time unnecessarily and still did not guard against overexposure/underexposure due to unpredictable changes in local tissue absorption, presence of bubbles, for example. Therefore, methods of real-time control of lesion formation which match the timescale of tissue modification and the small focal volumes in which therapeutic effects are taking place, would be of great value in terms of improving the safety and efficacy of therapeutic HIFU.

The real-time implementation of UST was made possible by streaming beamformed diagnostic ultrasound RF echo data to a GPU-based PC platform using a Gigabit interface [85]. This allowed real-time computation of the temperature change on the same RF grid, i.e. with approximately 18.75 μm axial spacing and 0.300 mm lateral spacing using the full frame rate of the ultrasound imaging system. This allowed the implementation of a closed-loop temperature control algorithm using a therapeutic array with an integrated diagnostic probe [137]. Spatial and temporal temperature feedback from a plane intersecting multiple-focus [98] heating patterns has been obtained using the real-time UST method described in [85]. The power deposition to two foci was adjusted to maintain the set-point temperatures at two distinct focal points for varying durations. The two-focus patterns were resynthesised 25 times per second based on real-time imaging data streamlined at 100 frames per second. Compared to closed-loop temperature control based on MRgFUS [138–142], USgFUS allows high spatial and temporal resolution of temperature control.

Curiel and Hynynen [143] used the change in stiffness during lesion formation as a control parameter to stop the application of HIFU during relatively long ($\sim$40 s) exposures. Using the system shown in Figure 3, *in vivo* results have shown that a threshold change in displacement is indicative of lesion formation and thus be used to stop the application of the therapeutic beam.

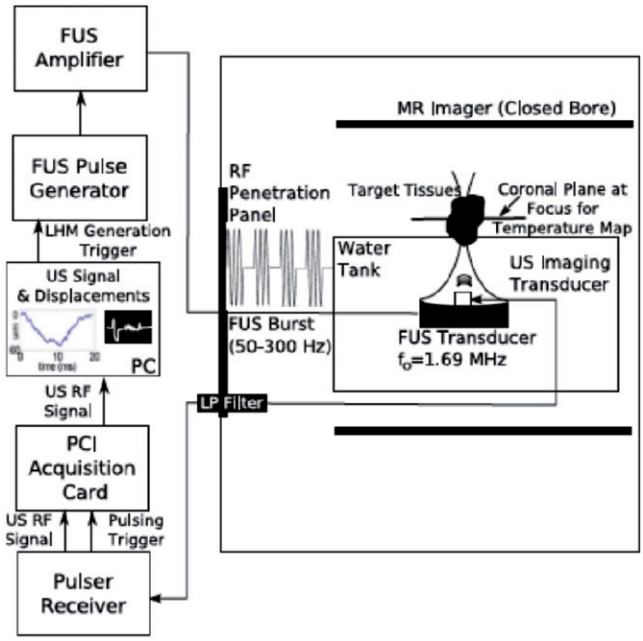

Figure 3. Schematic diagram of a USgFUS system designed for monitoring changes in lesion stiffness using localised harmonic motion (LHM). Reproduced with permission from Curiel et al. [143,178].

The use of dual-mode ultrasound array (DMUA) transducers [81,144–147] may provide an improved solution to lesion mapping based on echogenicity change. Using an integrated diagnostic probe with a DMUA transducer, Casper et al. [82] compared the area of a hyperechoic spot seen on DMUA and diagnostic probe images. Mapping obtained using DMUA images was consistent with the spatial extent of the HIFU-induced lesions. This improved mapping can be attributed to several factors, including 1) inherent registration between imaging and therapy beams, 2) high sensitivity to bubble activity due to the high array receive gain at the HIFU focus, and 3) high sensitivity to resonant bubble activity when performing both imaging and therapy in the same frequency band. Casper et al. [148] demonstrated the feasibility of using a dual-mode ultrasound transducer (DMUT) to achieve controlled lesion size based on the detection of changes in integrated back scattering from lesion location. Liu et al. have demonstrated the feasibility of controlling the production of multiple lesions using a similar DMUA prototype.

Damage assessment

Quantitative imaging of tissue property changes indicative of lesion formation, both at the single 'shot' and volumetric lesion levels, is essential for the ultimate success of any image-guided therapy. The nature of tissue changes after lesion formation using both thermal and non-thermal HIFU therapies are fairly well understood, and suggests several imaging modes for assessment, with and without the use of UCA.

Lizzi and co-workers [118] proposed radiation force methods for monitoring the change in stiffness during lesion

formation. Preliminary *ex vivo* results showed qualitative agreement in differentiating HIFU-treated lesions from normal tissue. Quantitative assessment is made difficult by the transient nature of tissue boiling in the HIFU-induced lesions [149]. Hynynen and co-workers also investigated the use of local harmonic motion (LHM) for monitoring and assessment [143], and reported success in using stiffness as an indicator of lesion formation *in vivo*. Examination of the HIFU exposure levels used during these experiments suggests that boiling was not a factor as the MR-measured temperature rise at the focus was ~30 °C for a 40-s exposure. Konofagou and co-workers have also investigated the use of LHM in monitoring and assessment. Recently they reported the use of this technique as a multi-parametric monitoring and assessment method of HIFU boiling *ex vivo* [150].

Fink and co-workers have used SWEI for quantitative assessment of thermal lesions [151]. They suggested the use of this method to image the stiffness (or shear modulus) not only for its temperature dependence, but also to give a measure of the thermal dose. The *ex vivo* results suggest that this approach is applicable to HIFU-induced lesions. It has also been used for damage assessment during histotripsy treatments [152,153]. In this case the tissue fractionation results in a 'softening' at the lesion location that can be detected with high sensitivity using SWEI. Significant reductions in Young's modulus have been reported after histotripsy in tissue-mimicking phantoms and *ex vivo* kidney.

Classical static elastography has also been suggested as a means of damage assessment, or of visualisation of HIFU-induced lesions [33,55,56,117,154].

It is known that tissue absorption changes with increased temperature, and after thermal lesion formation [155,156]. Ribault et al. [157] investigated the use of diagnostic ultrasound for measuring the change in local absorption as an indicator of lesion formation *ex vivo*. They reported a 'strong similarity' between the change in local absorption and the lesion volume 'as defined by the operator.' Liu and Ebbini [85] have demonstrated the use of sub-therapeutic HIFU exposures in measuring the change of relative absorption of *ex vivo* porcine heart after lesion formation. Their measurement also demonstrated the transient nature of tissue properties even minutes after lesion formation. This is illustrated in Figure 4, which shows the maximum temperature rise due to a sub-therapeutic FUS beam before (blue) and after (red) lesion formation due to a 5-s HIFU exposure. These results show that it took approximately 4 min for the absorption measurement to stabilise.

Kennedy et al. [89] proposed the use of UCA for immediate assessment of HIFU-induced damage in liver tumours. The use of contrast-enhanced ultrasound (CEUS) for this purpose is motivated by the known effects of damage to the vasculature in thermal therapy. The authors provided the first documentation of UCA delineation of the extent of HIFU ablation by comparing pre- and immediately post-treatment perfusion within the target (liver) tumour. These findings were backed up by histological evaluation of the treated volume.

USgFUS versus MRgFUS

The introduction of MRgFUS in the 1990s was a major factor in propelling therapeutic ultrasound to the exciting stage in which we find it today. The soft-tissue contrast achieved by MRI, together with the development of MR thermography [39,40] and elastography [43] have helped tremendously in convincing the clinical community. While USgFUS has been used since the early days of diagnostic ultrasound in the 1970s [37,158], the quality of B-mode imaging for the specific aspects of image guidance described in the previous section has been poor. However, several developments have occurred during the last two decades in ultrasound imaging that are helping to change the status of USgFUS. Examples of these developments (which include UCA imaging, elastography, thermography, ARFI and supersonic imaging, passive cavitation mapping) have already been described above. However, most of these are not yet clinically approved, and their use is currently limited to the research groups that invented/introduced them. It is expected that more widespread use of these methods will demonstrate their applicability to clinical procedures, and will help with the regulatory approval processes. Table 1 summarises the various specialised MRgFUS and USgFUS methods for imaging FUS-tissue interactions and their potential in clinical use. We note that the table is not about which guidance modality is better; it is about what is available to capture key bioeffects that may help advance the use of therapeutic applications of FUS. Depending on the nature of the treatment and on available resources, it may be beneficial to design image-guidance methods based on a combination of USgFUS and MRgFUS [159–161].

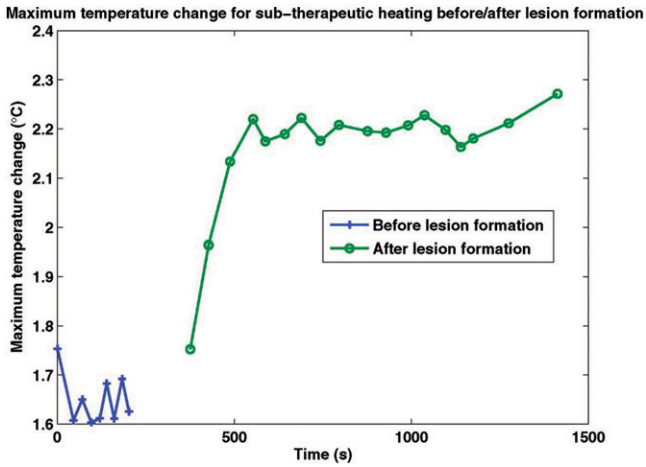

Figure 4. Maximum temperature change due to the application of 1.7-s sub-therapeutic HIFU 'shots' before and after the application of a 5-s therapeutic HIFU 'shot'. Reproduced from Liu and Ebbini [85] with permission.

Table 1 shows the HIFU-induced lesion parameters (or features) currently imaged using MRI and ultrasound. While both imaging modalities have been shown to provide useful imaging of HIFU-induced lesions, the superior soft-tissue contrast of MRI represents a major advantage in terms of specificity. Ultrasound has superior sensitivity to both thermal and mechanical effects in the presence of tissue motion and deformation, especially when high frame rates are utilised [82,84,85,114]. Its real-time nature is a major advantage when real-time closed-loop control of HIFU is required. The specificity of ultrasound imaging, including quantitative imaging, used in USgFUS will probably help to provide a

Table 1. FUS-induced lesion parameter imaging using MRgHIFU and USgHIFU.

	MRgHIFU		USgHIFU	
Feature/parameter to be imaged	Treatment planning	Real time treatment monitoring	Treatment planning	Real time treatment monitoring
Tumour boundaries	T1, T2, T2*, DWI	T1, T2, T2*, DWI	B-mode, CEUS	B-mode
Bone	T1, T2, T2*, DWI, UTE	T1, T2, T2*, DWI	B-mode	B-mode (greyscale changes in soft tissue surrounding bone)
Hypoxia	DWI, DCE	DWI, DCE	–	(CEUS)
Perfusion	DSC, DCE	DSC, DCE	CEUS	CEUS
Temperature	–	EPI, T2*	–	Speed of sound
	–	GRE	–	
Tissue changes		DWI, MR elastography	B-mode	B-mode (greyscale changes), Elastography, RFI, harmonic motion imaging

DWI, diffusion weighted imaging; UTE, ultrashort echo time; DCE, dynamic contrast enhanced imaging – requires gadolinium contrast agents so only used prior to treatment session or post-treatment; DSC, dynamic susceptibility contrast – only used in brain applications at present, requires gadolinium; EPI, echo planar imaging – fast acquisition, sensitive to susceptibility artefacts and magnetic field inhomogeneities; GRE, gradient recalled echo sequence – slower than EPI; CEUS, contrast enhanced ultrasound – uses microbubble contrast agents to provide scattering contrast.

major push towards a more widespread adoption of image-guided interventions.

Future trends in USgFUS

USgFUS has come a long way from simple B-mode visualisation of echogenic changes during, and immediately after, the application of HIFU. Numerous methods with much higher specificity to FUS, at therapeutic and sub-therapeutic levels, have been shown to be feasible. Undoubtedly, most of these methods will continue to develop and eventually prove worthy of clinical use for one or more aspects of image guidance: planning, siting, monitoring, control, and damage assessment. At this point, clinical USgFUS systems mainly use echogenicity change for feedback, but colour Doppler flow imaging (CDFI) has been used to identify the target in one renal denervation study [162]. This is an example of the use of multimodal ultrasound for image guidance that can offer ultrasound a unique real-time advantage.

The increased use of high performance computing (HPC) for beamforming and post-beamforming signal processing (e.g. GPUs [113,163,164]) is allowing the real-time implementation of demanding algorithms for image guidance, e.g. UST [85]. HPC has enabled the demonstration of real-time temperature control, including the re-synthesis of multiple-focus FUS patterns based on UST [137]. It is expected that, with real-time implementation of the aforementioned monitoring methods, real-time control based on monitoring will become routine in many applications. The myriad of closed-loop control algorithms developed for MRgFUS [39,138,142,165–168] offer a glimpse of what is coming in USgFUS. Of course, with USgFUS, the high frame-rate nature of ultrasound imaging will prove to be critical in some applications, such as cardiac ablation.

Advances in array transducer technology, together with HPC-based advanced beamforming and signal processing methods, will continue to shape USgFUS applications. Several examples of dual-mode ultrasound arrays have recently been described [82,146,169]. Piezocomposite transducer technologies [170] offer some design options that allow trade-offs between imaging and therapeutic performance. Capacitive micromachined ultrasonic transducer (CMUT) arrays [171] represent another promising technology that is expected to provide additional design options for DMUA-based USgFUS approaches.

The advent of real-time 3D ultrasound and its use in USgFUS [172] may prove to be the key to overcoming a major limitation of this image guidance modality. It is well known that out-of-plane motion could negatively impact USgFUS methods such as thermography, elastography, SWEI, for example. Using 3D imaging in conjunction with these methods could be the answer in applications involving high levels of 3D motion and deformation. Although currently focused on echogenicity changes [172], it is expected that other forms of more quantitative 3D imaging will be developed in the near future [173]. This includes 3D speckle tracking [174], which will help to improve the robustness of ultrasound thermography and elastography.

Where appropriate, combining USgFUS and MRgFUS may also prove essential for improving the safety and efficacy of the therapeutic application of FUS. This has been suggested in some publications [159,161] and has been suggested in related applications such as image-guided RF ablation [175,176].

Conclusions

It is clear that advances in medical ultrasound such as elastography, CEUS, SWEI, thermography and ultrafast imaging are applicable for the guidance of FUS. We have discussed examples of the use of these methods in all aspects of image guidance, including pretreatment planning, focus siting, monitoring, control, and damage assessment. The adoption of GPU-based beamforming and signal processing has led to laboratory demonstration of the feasibility of most of these methods, which bodes well for their adoption in the clinic.

This review has also demonstrated that many of the ultrasound imaging methods developed for USgFUS are maturing with their real-time, *in vivo* demonstration [65,85,89,114,143,177]. The growing awareness of these important results can be expected to increase the momentum towards clinical adoption of ultrasound as a guidance method.

A comparison between USgFUS and MRgFUS shows that both modalities offer options for all aspects of image guidance. MRgFUS offers some clear advantages in terms of lesion visualisation and, in some cases, clinical implementation of real-time thermography. For maximum patient safety and treatment efficacy it is clear that USgFUS may be adequate, for example in transrectal HIFU for prostatic cancer [154]. On the other hand, applications involving transcranial FUS [44] currently require MRgFUS. This may change with more advanced ultrasound image reconstruction and aberration corrections, but it may also be useful to combine both modalities in some applications.

In summary, USgFUS is gaining momentum towards wider clinical adoption. This review provides a snapshot of a burgeoning field on the verge of another revolution in medical technology. The developments in quantitative, high-resolution USgFUS methods will likely lead to unprecedented levels of safety and efficacy in image-guided 'bloodless' interventions.

Declaration of interest

The authors report no conflicts of interest. The authors alone are responsible for the content and writing of the paper.

References

1. Fry WJ. Intense ultrasound: A new tool for neurological research. J Ment Sci 1954;100:85–96.
2. Barnard JW, Fry WJ, Fry FJ, Brennan JF. Small localized ultrasonic lesions in the white and gray matter of the cat brain. AMA Arch Neurol Psychiatry 1956;75:15–35.
3. Fry WJ. Ultrasound in neurology. Neurology 1956;6:693–704.
4. Fry WJ, Barnard JW, Fry EJ, Krumins RF, Brennan JF. Ultrasonic lesions in the mammalian central nervous system. Science 1955; 122:517–18.
5. Basauri L, Lele PP. A simple method for production of trackless focal lesions with focused ultrasound: Statistical evaluation of the effects of irradiation on the central nervous system of the cat. J Physiol 1962;160:513–34.
6. Frizzell LA. Threshold dosages for damage to mammalian liver by high intensity focused ultrasound. IEEE Trans Ultrason Ferroelectr Freq Control 1988;35:578–81.
7. Hynynen K. The threshold for thermally significant cavitation in dogs thigh muscle in vivo. Ultrasound Med Biol 1991;17:157–69.
8. Fry FJ, Kossoff G, Eggleton RC, Dunn F. Threshold ultrasonic dosages for structural changes in the mammalian brain. J Acoust Soc Am 1970;48:1413–17.
9. Sapareto SA, Dewey WC. Thermal dose determination in cancer therapy. Int J Radiat Oncol Biol Phys 1984;10:787–800.
10. Engel DJ, Muratore R, Hirata K, Otsuka R, Fujikura K, Sugioka K, et al. Myocardial lesion formation using high-intensity focused ultrasound. J Am Soc Echocardiogr 2006;19:932–7.
11. Lele PP. Induction of deep, local hyperthermia by ultrasound and electromagnetic fields: problems and choices. Radiat Environ Biophys 1980;17:205–17.
12. Lele PP. Local tumor hyperthermia in the 1990s. Adv Exp Med Biol 1990;267:37–46.
13. Lele PP. Advanced ultrasonic techniques for local tumor hyperthermia. Radiol Clin North Am 1989;27:559–75.
14. Jia ZQ, Worthington AE, Hill RP, Hunt JW. The effects of artery occlusion on temperature homogeneity during hyperthermia in rabbit kidneys in vivo. Int J Hyperthermia 1997;13:21–37.
15. Hynynen K, Watmough DJ, Mallard JR, Fuller M. Local hyperthermia induced by focussed and overlapping ultrasonic fields – An in vivo demonstration. Ultrasound Med Biol 1983;9:621–7.
16. Tobias J, Hynynen K, Roemer R, Guthkelch AN, Fleischer AS, Shively J. An ultrasound window to perform scanned, focused ultrasound hyperthermia treatments of brain tumors. Med Phys 1987;14:228–34.
17. Hynynen K, Roemer R, Anhalt D, Johnson C, Xu ZX, Swindell W, et al. A scanned, focused, multiple transducer ultrasonic system for localized hyperthermia treatments. Int J Hyperthermia 1987;3: 21–35.
18. Shimm DS, Hynynen KH, Anhalt DP, Roemer RB, Cassady JR. Scanned focussed ultrasound hyperthermia: initial clinical results. Int J Radiat Oncol Biol Phys 1988;15:1203–8.
19. Benkeser PJ, Frizzell LA, Ocheltree KB, Cain CA. A tapered phased array ultrasound transducer for hyperthermia treatment. IEEE Trans Ultrason Ferroelectr Freq Control 1987;34:446–53.
20. Ebbini ES, Umemura SI, Ibbini M, Cain CA. A cylindrical-section ultrasound phased-array applicator for hyperthermia cancer therapy. IEEE Trans Ultrason Ferroelectr Freq Control 1988;35:561–72.
21. Lele PP. In: Storm FK, ed. Hyperthermia Cancer Therapy. Boston, MA: GK Hall, 1983.
22. Hunt JW, Lalonde R, Ginsberg H, Urchuk S, Worthington A. Rapid heating: Critical theoretical assessment of thermal gradients found in hyperthermia treatments. Int J Hyperthermia 1991;7:703–18.
23. Farny CH, Holt RG, Roy RA. The correlation between bubble-enhanced HIFU heating and cavitation power. IEEE Trans Biomed Eng 2010;57:175–84.
24. Roberts WW, Hall TL, Ives K, Wolf Jr JS, Fowlkes JB, Cain CA. Pulsed cavitational ultrasound: A noninvasive technology for controlled tissue ablation (histotripsy) in the rabbit kidney. J Urol 2006;175:734–8.
25. Lake AM, Hall TL, Kieran K, Fowlkes JB, Cain CA, Roberts WW. Histotripsy: Minimally invasive technology for prostatic tissue ablation in an in vivo canine model. Urology 2008;72:682–6.
26. Lake AM, Xu Z, Wilkinson JE, Cain CA, Roberts WW. Renal ablation by histotripsy – Does it spare the collecting system? J Urol 2008;179:1150–4.
27. Maxwell AD, Cain CA, Duryea AP, Yuan L, Gurm HS, Xu Z. Noninvasive thrombolysis using pulsed ultrasound cavitation therapy – Histotripsy. Ultrasound Med Biol 2009;35:1982–94.
28. Xu Z, Owens G, Gordon D, Cain C, Ludomirsky A. Noninvasive creation of an atrial septal defect by histotripsy in a canine model. Circulation 2010;121:742–9.
29. Wang YN, Khokhlova T, Bailey M, Hwang JH, Khokhlova V. Histological and biochemical analysis of mechanical and thermal bioeffects in boiling histotripsy lesions induced by high intensity focused ultrasound. Ultrasound Med Biol 2013;39:424–38.
30. Hill CR, ter Haar GR. Review article: High intensity focused ultrasound –Potential for cancer treatment. Br J Radiol 1995;68: 1296–303.
31. Rowland IJ, Rivens I, Chen L, Lebozer CH, Collins DJ, ter Haar GR, et al. MRI study of hepatic tumours following high intensity focused ultrasound surgery. Br J Radiol 1997;70:144–53.
32. ter Haar GR. High intensity focused ultrasound for the treatment of tumors. Echocardiography 2001;18:317–22.
33. Souchon R, Rouviere O, Gelet A, Detti V, Srinivasan S, Ophir J, et al. Visualisation of HIFU lesions using elastography of the human prostate in vivo: Preliminary results. Ultrasound Med Biol 2003;29:1007–15.
34. ter Haar G. Therapeutic ultrasound. Eur J Ultrasound 1999;9:3–9.
35. Vaezy S, Martin R, Yaziji H, Kaczkowski P, Keilman G, Carter S, et al. Hemostasis of punctured blood vessels using high-intensity focused ultrasound. Ultrasound Med Biol 1998;24:903–10.
36. Yang R, Sanghvi NT, Rescorla FJ, Galliani CA, Fry FJ, Griffith SL, et al. Extracorporeal liver ablation using sonography-guided high-intensity focused ultrasound. Invest Radiol 1992;27:796–803.
37. Coleman DJ, Rondeau MJ, Silverman RH, Lizzi FL. Computerized ultrasonic biometry and imaging of intraocular tumors for the monitoring of therapy. Trans Am Ophthalmol Soc 1987;85:49–81.
38. Bush NL, Rivens I, ter Haar GR, Bamber JC. Acoustic properties of lesions generated with an ultrasound therapy system. Ultrasound Med Biol 1993;19:789–801.
39. Hutchinson E, Dahleh M, Hynynen K. The feasibility of MRI feedback control for intracavitary phased array hyperthermia treatments. Int J Hyperthermia 1998;14:39–56.
40. McDannold NJ, King RL, Jolesz FA, Hynynen KH. Usefulness of MR imaging-derived thermometry and dosimetry in determining the threshold for tissue damage induced by thermal surgery in rabbits. Radiology 2000;216:517–23.
41. Wharton IP, Rivens IH, ter Haar GR, Gilderdale DJ, Collins DJ, Hand JW, et al. Design and development of a prototype

endocavitary probe for high-intensity focused ultrasound delivery with integrated magnetic resonance imaging. J Magn Reson Imaging 2007;25:548–56.
42. Leslie TA, Kennedy JE, Illing RO, ter Haar GR, Wu F, Phillips RR, et al. High-intensity focused ultrasound ablation of liver tumours: Can radiological assessment predict the histological response?. Br J Radiol 2008;81:564–71.
43. Kaye EA, Chen J, Pauly KB. Rapid MR-ARFI method for focal spot localization during focused ultrasound therapy. Magn Reson Med 2011;65:738–43.
44. McDannold N, Vykhodtseva N, Jolesz FA, Hynynen K. MRI investigation of the threshold for thermally induced blood–brain barrier disruption and brain tissue damage in the rabbit brain. Magn Reson Med 2004;51:913–23.
45. Parker DL, Smith V, Sheldon P, Crooks LE, Fussell L. Temperature distribution measurements in two-dimensional NMR imaging. Med Phys 1983;10:321–5.
46. Parker DL. Applications of NMR imaging in hyperthermia: An evaluation of the potential for localized tissue heating and noninvasive temperature monitoring. IEEE Trans Biomed Eng 1984;31:161–7.
47. Seip R, Ebbini ES. Noninvasive estimation of tissue temperature response to heating fields using diagnostic ultrasound. IEEE Trans Biomed Eng 1995;42:828–39.
48. Simon C, Vanbaren P, Ebbini ES. Two-dimensional temperature estimation using diagnostic ultrasound. IEEE Trans Ultrason Ferroelectr Freq Control 1998;45:1088–99.
49. Arthur RM, Straube WL, Starman JD, Moros EG. Noninvasive temperature estimation based on the energy of backscattered ultrasound. Med Phys 2003;30:1021–9.
50. Arthur RM, Trobaugh JW, Straube WL, Moros EG. Temperature dependence of ultrasonic backscattered energy in motion-compensated images. IEEE Trans Ultrason Ferroelectr Freq Control 2005; 52:1644–52.
51. Arthur RM, Straube WL, Trobaugh JW, Moros EG. In vivo change in ultrasonic backscattered energy with temperature in motion-compensated images. Int J Hyperthermia 2008;24:389–98.
52. Maass-Moreno R, Damianou CA, Sanghvi NT. Noninvasive temperature estimation in tissue via ultrasound echo-shifts. Part II. In vitro study. J Acoust Soc Am 1996;100:2522–30.
53. Maass-Moreno R, Damianou CA. Noninvasive temperature estimation in tissue via ultrasound echo-shifts. Part I. Analytical model. J Acoust Soc Am 1996;100:2514–21.
54. Chen J, Watkins R, Pauly KB. Optimization of encoding gradients for MR-ARFI. Magn Reson Med 2010;63:1050–8.
55. Righetti R, Kallel F, Stafford RJ, Price RE, Krouskop TA, Hazle JD, et al. Elastographic characterization of HIFU-induced lesions in canine livers. Ultrasound Med Biol 1999;25: 1099–113.
56. Kallel F, Stafford RJ, Price RE, Righetti R, Ophir J, Hazle JD. The feasibility of elastographic visualization of HIFU-induced thermal lesions in soft tissues. Image-guided high-intensity focused ultrasound. Ultrasound Med Biol 1999;25:641–7.
57. Souchon R, Soualmi L, Bertrand M, Chapelon JY, Kallel F, Ophir J. Ultrasonic elastography using sector scan imaging and a radial compression. Ultrasonics 2002;40:867–71.
58. Souchon R, Salomir R, Beuf O, Milot L, Grenier D, Lyonnet D, et al. Transient MR elastography (t-MRE) using ultrasound radiation force: Theory, safety, and initial experiments in vitro. Magn Reson Med 2008;60:871–81.
59. Rouviere O, Souchon R, Pagnoux G, Menager JM, Chapelon JY. Magnetic resonance elastography of the kidneys: Feasibility and reproducibility in young healthy adults. J Magn Reson Imaging 2011;34:880–6.
60. Moros EG, Dutton AW, Roemer RB, Burton M, Hynynen K. Experimental evaluation of two simple thermal models using hyperthermia in muscle in vivo. Int J Hyperthermia 1993;9: 581–98.
61. Meaney PM, Clarke RLter Haar GR, Rivens IH. A 3-D finite-element model for computation of temperature profiles and regions of thermal damage during focused ultrasound surgery exposures. Ultrasound Med Biol 1998;24:1489–99.
62. Meaney PM, Cahill MD, ter Haar GR. The intensity dependence of lesion position shift during focused ultrasound surgery. Ultrasound Med Biol 2000;26:441–50.
63. Swindell W. A theoretical study of nonlinear effects with focused ultrasound in tissues: an acoustic bragg peak. Ultrasound Med Biol 1985;11:121–30.
64. Chavrier F, Chapelon JY, Gelet A, Cathignol D. Modeling of high-intensity focused ultrasound-induced lesions in the presence of cavitation bubbles. J Acoust Soc Am 2000; 108:432–40.
65. Shehata IA, Ballard JR, Casper AJ, Liu D, Mitchell T, Ebbini ES. Feasibility of targeting atherosclerotic plaques by high-intensity-focused ultrasound: An in vivo study. J Vasc Interv Radiol 2013;24: 1880–7.
66. Dupuy DE, Goldberg SN. Image-guided radiofrequency tumor ablation: challenges and opportunities – Part II. J Vasc Interv Radiol 2001;12:1135–48.
67. Ahmed M, Solbiati L, Brace CL, Breen DJ, Callstrom MR, Charboneau JW, et al. Image-guided tumor ablation: Standardization of terminology and reporting criteria – A 10-year update. Radiology 2014;273:241–60.
68. Ebbini ES, Cain CA. Optimization of the intensity gain of multiple-focus phased-array heating patterns. Int J Hyperthermia 1991;7: 953–73.
69. Ebbini ES, Cain CA. A spherical-section ultrasound phased array applicator for deep localized hyperthermia. IEEE Trans Biomed Eng 1991;38:634–43.
70. Lele PP. Effect of Ultrasound on solid mammalian tissues and tumros in vivo. In: Repacholi MGH, Rindi M, Ed A, eds. Ultrasound: Medical Applications, Biological Effects and Hazzard Potential. New York: Plenum, 1987.
71. Hall TL, Kieran K, Ives K, Fowlkes JB, Cain CA, Roberts WW. Histotripsy of rabbit renal tissue in vivo: Temporal histologic trends. J Endourol 2007;21:1159–66.
72. Palmeri ML, Miller ZA, Glass TJ, Garcia-Reyes K, Gupta RT, Rosenzweig SJ, et al. B-mode and acoustic radiation force impulse (ARFI) imaging of prostate zonal anatomy: Comparison with 3T T2-weighted MR imaging. Ultrason Imaging 2014;37:22–41.
73. Gallippi CM, Nightingale KR, Trahey GE. BSS-based filtering of physiological and ARFI-induced tissue and blood motion. Ultrasound Med Biol 2003;29:1583–92.
74. Sarvazyan AP, Rudenko OV, Swanson SD, Fowlkes JB, Emelianov SY. Shear wave elasticity imaging: A new ultrasonic technology of medical diagnostics. Ultrasound Med Biol 1998;24:1419–35.
75. Ostrovsky L, Sutin A, Ilinskii Y, Rudenko O, Sarvazyan A. Radiation force and shear motions in inhomogeneous media. J Acoust Soc Am 2007;121:1324–31.
76. Sandrin L, Tanter M, Catheline S, Fink M. Shear modulus imaging with 2-D transient elastography. IEEE Trans Ultrason Ferroelectr Freq Control 2002;49:426–35.
77. Bercoff J, Tanter M, Fink M. Supersonic shear imaging: A new technique for soft tissue elasticity mapping. IEEE Trans Ultrason Ferroelectr Freq Control 2004;51:396–409.
78. Livneh A, Kimmel E, Kohut AR, Adam D. Extracorporeal acute cardiac pacing by high intensity focused ultrasound. Prog Biophys Mol Biol 2014;115:140–53.
79. Dalecki D, Raeman CH, Child SZ, Carstensen EL. Effects of pulsed ultrasound on the frog heart: III. The radiation force mechanism. Ultrasound Med Biol 1997;23:275–85.
80. Gyongy M, Coussios CC. Passive spatial mapping of inertial cavitation during HIFU exposure. IEEE Trans Biomed Eng 2010; 57:48–56.
81. Ebbini ES, Yao H, Shrestha A. Dual-mode ultrasound phased arrays for image-guided surgery. Ultrason Imaging 2006;28: 65–82.
82. Casper AJ, Liu D, Ballard JR, Ebbini ES. Real-time implementation of a dual-mode ultrasound array system: in vivo results. IEEE Trans Biomed Eng 2013;60:2751–9.
83. Simpson DH, Chin CT, Burns PN. Pulse inversion Doppler: A new method for detecting nonlinear echoes from microbubble contrast agents. IEEE Trans Ultrason Ferroelectr Freq Control 1999;46: 372–82.
84. Gateau J, Aubry JF, Pernot M, Fink M, Tanter M. Combined passive detection and ultrafast active imaging of cavitation events induced by short pulses of high-intensity ultrasound. IEEE Trans Ultrason Ferroelectr Freq Control 2011;58:517–32.
85. Liu D, Ebbini ES. Real-time 2-D temperature imaging using ultrasound. IEEE Trans Biomed Eng 2010;57:12–16.

86. Treat LH, McDannold N, Zhang Y, Vykhodtseva N, Hynynen K. Improved anti-tumor effect of liposomal doxorubicin after targeted blood–brain barrier disruption by MRI-guided focused ultrasound in rat glioma. Ultrasound Med Biol 2012;38:1716–25.
87. Park SM, Kim MS, Park SJ, Park ES, Choi KS, Kim YS, et al. Novel temperature-triggered liposome with high stability: Formulation, in vitro evaluation, and in vivo study combined with high-intensity focused ultrasound (HIFU). J Control Release 2013;170:373–9.
88. Poliachik SL, Chandler WL, Mourad PD, Bailey MR, Bloch S, Cleveland RO, et al. Effect of high-intensity focused ultrasound on whole blood with and without microbubble contrast agent. Ultrasound Med Biol 1999;25:991–8.
89. Kennedy JE, ter Haar GR, Wu F, Gleeson FV, Roberts IS, Middleton MR, et al. Contrast-enhanced ultrasound assessment of tissue response to high-intensity focused ultrasound. Ultrasound Med Biol 2004;30:851–4.
90. Kennedy JE, Wu F, ter Haar GR, Gleeson FV, Phillips RR, Middleton MR, et al. High-intensity focused ultrasound for the treatment of liver tumours. Ultrasonics 2004;42:931–5.
91. Rahim AA, Taylor SL, Bush NL, ter Haar GR, Bamber JC, Porter CD. Spatial and acoustic pressure dependence of microbubble-mediated gene delivery targeted using focused ultrasound. J Gene Med 2006;8:1347–57.
92. Rahim A, Taylor SL, Bush NL, ter Haar GR, Bamber JC, Porter CD. Physical parameters affecting ultrasound/microbubble-mediated gene delivery efficiency in vitro. Ultrasound Med Biol 2006;32:1269–79.
93. Hynynen K, McDannold N, Vykhodtseva N, Jolesz FA. Noninvasive MR imaging-guided focal opening of the blood–brain barrier in rabbits. Radiology 2001;220:640–6.
94. Zhang M, Fabiilli ML, Haworth KJ, Fowlkes JB, Kripfgans OD, Roberts WW, et al. Initial investigation of acoustic droplet vaporization for occlusion in canine kidney. Ultrasound Med Biol 2010;36:1691–703.
95. Zhang M, Fabiilli ML, Haworth KJ, Padilla F, Swanson SD, Kripfgans OD, et al. Acoustic droplet vaporization for enhancement of thermal ablation by high intensity focused ultrasound. Acad Radiol 2011;18:1123–32.
96. Hynynen K, DeYoung D. Temperature elevation at muscle–bone interface during scanned, focused ultrasound hyperthermia. Int J Hyperthermia 1988;4:267–79.
97. Moros EG, Roemer RB, Hynynen K. Simulations of scanned focused ultrasound hyperthermia. The effects of scanning speed and pattern on the temperature fluctuations at the focal depth. IEEE Trans Ultrason Ferroelectr Freq Control 1988;35:552–60.
98. Ebbini ES, Cain CA. Multiple-focus ultrasound phased-array pattern synthesis: optimal driving-signal distributions for hyperthermia. IEEE Trans Ultrason Ferroelectr Freq Control 1989;36:540–8.
99. Hynynen K. Hot spots created at skin–air interfaces during ultrasound hyperthermia. Int J Hyperthermia 1990;6:1005–12.
100. Fan X, Hynynen K. The effect of wave reflection and refraction at soft tissue interfaces during ultrasound hyperthermia treatments. J Acoust Soc Am 1992;91:1727–36.
101. Lin WL, Roemer RB, Moros EG, Hynynen K. Optimization of temperature distributions in scanned, focused ultrasound hyperthermia. Int J Hyperthermia 1992;8:61–78.
102. McGough RJ, Ebbini ES, Cain CA. Direct computation of ultrasound phased-array driving signals from a specified temperature distribution for hyperthermia. IEEE Trans Biomed Eng 1992;39:825–35.
103. Sun J, Hynynen K. The potential of transskull ultrasound therapy and surgery using the maximum available skull surface area. J Acoust Soc Am 1999;105:2519–27.
104. Clement GT, Sun J, Hynynen K. The role of internal reflection in transskull phase distortion. Ultrasonics 2001;39:109–13.
105. Aubry JF, Tanter M, Pernot M, Thomas JL, Fink M. Experimental demonstration of noninvasive transskull adaptive focusing based on prior computed tomography scans. J Acoust Soc Am 2003;113:84–93.
106. Botros YY, Volakis JL, VanBaren P, Ebbini ES. A hybrid computational model for ultrasound phased-array heating in presence of strongly scattering obstacles. IEEE Trans Biomed Eng 1997;44:1039–50.
107. Botros YY, Ebbini ES, Volakis JL. Two-step hybrid virtual array ray (VAR) technique for focusing through the rib cage. IEEE Trans Ultrason Ferroelectr Freq Control 1998;45:989–1000.
108. Gelat P, ter Haar G, Saffari N. Modelling of the acoustic field of a multi-element HIFU array scattered by human ribs. Phys Med Biol 2011;56:5553–81.
109. Gelat P, Ter Haar G, Saffari N. A comparison of methods for focusing the field of a HIFU array transducer through human ribs. Phys Med Biol 2014;59:3139–71.
110. Bobkova S, Gavrilov L, Khokhlova V, Shaw A, Hand J. Focusing of high-intensity ultrasound through the rib cage using a therapeutic random phased array. Ultrasound Med Biol 2010;36:888–906.
111. Almekkawy M. Optimization of focused ultrasound and image based modeling in image guided interventions [doctoral dissertation]. Department of Electrical and Computer Engineering, University of Minnesota, Minneapolis, 2014.
112. Civale J, Rivens I, ter Haar G, Morris H, Coussios C, Friend P, et al. Calibration of ultrasound backscatter temperature imaging for high-intensity focused ultrasound treatment planning. Ultrasound Med Biol 2013;39:1596–612.
113. Liu D, Ebbini ES. Real-time two-dimensional temperature imaging using ultrasound. Conf Proc IEEE Eng Med Biol Soc 2009;2009:1971–4. DOI: 10.1109/IEMBS.2009.533344.
114. Bayat MB, Ballard J, Ebbini E. In vivo ultrasound thermography in presence of temperature heterogeneity and natural motions. IEEE Trans Biomed Eng 2014;99. doi:10.1109/TBME.2014.2358075.
115. Vyas U, Kaye E, Pauly KB. Transcranial phase aberration correction using beam simulations and MR-ARFI. Med Phys 2014;41. p 032901.
116. Dumont DM, Doherty JR, Trahey GE. Noninvasive assessment of wall-shear rate and vascular elasticity using combined ARFI/SWEI/spectral Doppler imaging system. Ultrason Imaging 2011;33:165–88.
117. Alaniz A, Kallel F, Hungerford E, Ophir J. Variational method for estimating the effects of continuously varying lenses in HIFU, sonography, and sonography-based cross-correlation methods. J Acoust Soc Am 2002;111:468–74.
118. Lizzi FL, Muratore R, Deng CX, Ketterling JA, Alam SK, Mikaelian S, et al. Radiation-force technique to monitor lesions during ultrasonic therapy. Ultrasound Med Biol 2003;29:1593–605.
119. Bercoff J, Pernot M, Tanter M, Fink M. Monitoring thermally-induced lesions with supersonic shear imaging. Ultrason Imaging 2004;26:71–84.
120. Rabkin BA, Zderic V, Crum LA, Vaezy S. Biological and physical mechanisms of HIFU-induced hyperecho in ultrasound images. Ultrasound Med Biol 2006;32:1721–9.
121. Kyriakou Z, Corral-Baques MI, Amat A, Coussios CC. HIFU-induced cavitation and heating in ex vivo porcine subcutaneous fat. Ultrasound Med Biol 2011;37:568–79.
122. Haworth K, Salgaonkar VA, Corregan NM, Holland CK, Mast TD. Spatial specificity and sensitivity of passive cavitation imaging for monitoring high-intensity focused ultrasound thermal ablation in ex vivo bovine liver. Proc Meet Acoust 2013;19:075022.
123. Li T, Chen H, Khokhlova T, Wang YN, Kreider W, He X, et al. Passive cavitation detection during pulsed HIFU exposures of ex vivo tissues and in vivo mouse pancreatic tumors. Ultrasound Med Biol 2014;40:1523–34.
124. ter Haar G, Sinnett D, Rivens I. High intensity focused ultrasound – A surgical technique for the treatment of discrete liver tumours. Phys Med Biol 1989;34:1743–50.
125. Vaezy S, Shi X, Martin RW, Chi E, Nelson PI, Bailey MR, et al. Real-time visualization of high-intensity focused ultrasound treatment using ultrasound imaging. Ultrasound Med Biol 2001;27:33–42.
126. Illing RO, Kennedy JE, Wu F, ter Haar GR, Protheroe AS, Friend PJ, et al. The safety and feasibility of extracorporeal high-intensity focused ultrasound (HIFU) for the treatment of liver and kidney tumours in a Western population. Br J Cancer 2005;93:890–5.

127. Wu F, ter Haar G, Chen WR. High-intensity focused ultrasound ablation of breast cancer. Expert Rev Anticancer Ther 2007;7: 823–31.
128. McLaughlan J, Rivens I, Leighton T, ter Haar G. A study of bubble activity generated in ex vivo tissue by high intensity focused ultrasound. Ultrasound Med Biol 2010;36:1327–44.
129. Phukpattaranont P, Ebbini ES. Post-beamforming second-order Volterra filter for pulse-echo ultrasonic imaging. IEEE Trans Ultrason Ferroelectr Freq Control 2003;50:987–1001.
130. Straube WL, Arthur RM. Theoretical estimation of the temperature dependence of backscattered ultrasonic power for noninvasive thermometry. Ultrasound Med Biol 1994;20:915–22.
131. Matsuzawa R, Shishitani T, Yoshizawa T, Umemura S. Monitoring of lesion induced by high-intensity focused ultrasound using correlation method based on block matching. Jpn J Appl Phys 2012;51:1–6.
132. Subramanian S, Rudich SM, Alqadah A, Karunakaran CP, Rao MB, Mast TD. In vivo thermal ablation monitoring using ultrasound echo decorrelation imaging. Ultrasound Med Biol 2014;40:102–14.
133. Coussios CC, Farny CH, Haar GT, Roy RA. Role of acoustic cavitation in the delivery and monitoring of cancer treatment by high-intensity focused ultrasound (HIFU). Int J Hyperthermia 2007;23:105–20.
134. Salgaonkar VA, Datta S, Holland CK, Mast TD. Passive cavitation imaging with ultrasound arrays. J Acoust Soc Am 2009;126: 3071–83.
135. Gyongy M, Coussios CC. Passive cavitation mapping for localization and tracking of bubble dynamics. J Acoust Soc Am 2010; 128:EL175–80.
136. Hill CR, Rivens I, Vaughan MG, ter Haar GR. Lesion development in focused ultrasound surgery: A general model. Ultrasound Med Biol 1994;20:259–69.
137. Casper A, Liu D, Ebbini ES. Realtime control of multiple-focus phased array heating patterns based on noninvasive ultrasound thermography. IEEE Trans Biomed Eng 2012;59:95–105.
138. Vimeux FC, De Zwart JA, Palussiere J, Fawaz R, Delalande C, Canioni P, et al. Real-time control of focused ultrasound heating based on rapid MR thermometry. Invest Radiol 1999;34: 190–3.
139. Salomir R, Vimeux FC, de Zwart JA, Grenier N, Moonen CT. Hyperthermia by MR-guided focused ultrasound: accurate temperature control based on fast MRI and a physical model of local energy deposition and heat conduction. Magn Reson Med 2000; 43:342–7.
140. Mougenot C, Salomir R, Palussiere J, Grenier N, Moonen CT. Automatic spatial and temporal temperature control for MR-guided focused ultrasound using fast 3D MR thermometry and multispiral trajectory of the focal point. Magn Reson Med 2004; 52:1005–15.
141. Moonen CT. Spatio-temporal control of gene expression and cancer treatment using magnetic resonance imaging-guided focused ultrasound. Clin Cancer Res 2007;13:3482–9.
142. Mougenot C, Quesson B, de Senneville BD, de Oliveira PL, Sprinkhuizen S, Palussiere J, et al. Three-dimensional spatial and temporal temperature control with MR thermometry-guided focused ultrasound (MRgHIFU). Magn Reson Med 2009;61: 603–14.
143. Curiel L, Chopra R, Hynynen K. In vivo monitoring of focused ultrasound surgery using local harmonic motion. Ultrasound Med Biol 2009;35:65–78.
144. Ballard JR, Casper AJ, Ebbini ES. Monitoring and guidance of HIFU beams with dual-mode ultrasound arrays. Conf Proc IEEE Eng Med Biol Soc 2009;2009:137–40.
145. Makin IR, Mast TD, Faidi W, Runk MM, Barthe PG, Slayton MH. Miniaturized ultrasound arrays for interstitial ablation and imaging. Ultrasound Med Biol 2005;31:1539–50.
146. Mast TD, Barthe PG, Makin IR, Slayton MH, Karunakaran CP, Burgess MT, et al. Treatment of rabbit liver cancer in vivo using miniaturized image-ablate ultrasound arrays. Ultrasound Med Biol 2011;37:1609–21.
147. Bouchoux G, Lafon C, Berriet R, Chapelon JY, Fleury G, Cathignol D. Dual-mode ultrasound transducer for image-guided interstitial thermal therapy. Ultrasound Med Biol 2008; 34:607–16.
148. Casper A, Haritonova A., Wilken-Resman E., Ebbini E. Robust detection and control of bubble activity during high intensity focused ultrasound ablation. IEEE InT Ultrason Symp 2012; 2615–18. DOI: 10.1109/ULTSYM.2012.0655.
149. Yao H, Ebbini E. Real-time monitoring of the transients of HIFU-induced lesions. IEEE Int Ultrason Symp 2003;2:1006–9.
150. Hou GY, Marquet F, Wang S, Konofagou EE. Multi-parametric monitoring and assessment of high-intensity focused ultrasound (HIFU) boiling by harmonic motion imaging for focused ultrasound (HMIFU): An ex vivo feasibility study. Phys Med Biol 2014;59:1121–45.
151. Sapin-de Brosses E, Gennisson JL, Pernot M, Fink M, Tanter M. Temperature dependence of the shear modulus of soft tissues assessed by ultrasound. Phys Med Biol 2010;55:1701–18.
152. Tanter M, Bercoff J, Athanasiou A, Deffieux T, Gennisson JL, Montaldo G, et al. Quantitative assessment of breast lesion viscoelasticity: Initial clinical results using supersonic shear imaging. Ultrasound Med Biol 2008;34:1373–86.
153. Wang TY, Hall TL, Xu Z, Fowlkes JB, Cain CA. Imaging feedback of histotripsy treatments using ultrasound shear wave elastography. IEEE Trans Ultrason Ferroelectr Freq Control 2012; 59:1167–81.
154. Curiel L, Souchon R, Rouviere O, Gelet A, Chapelon JY. Elastography for the follow-up of high-intensity focused ultrasound prostate cancer treatment: Initial comparison with MRI. Ultrasound Med Biol 2005;31:1461–8.
155. Kemmerer JP, Oelze ML. Ultrasonic assessment of thermal therapy in rat liver. Ultrasound Med Biol 2012;38:2130–7.
156. Damianou CA, Sanghvi NT, Fry FJ, Maass-Moreno R. Dependence of ultrasonic attenuation and absorption in dog soft tissues on temperature and thermal dose. J Acoust Soc Am 1997; 102:628–34.
157. Ribault M, Chapelon JY, Cathignol D, Gelet A. Differential attenuation imaging for the characterization of high intensity focused ultrasound lesions. Ultrason Imaging 1998;20: 160–77.
158. Coleman DJ, Lizzi FL, Burgess SE, Silverman RH, Smith ME, Driller J, et al. Ultrasonic hyperthermia and radiation in the management of intraocular malignant melanoma. Am J Ophthalmol 1986;101:635–42.
159. Auboiroux V, Petrusca L, Viallon M, Goget T, Becker CD, Salomir R. Ultrasonography-based 2D motion-compensated HIFU sonication integrated with reference-free MR temperature monitoring: A feasibility study ex vivo. Phys Med Biol 2012;57: N159–71.
160. Leslie T, Ritchie R, Illing R, ter Haar G, Phillips R, Middleton M, et al. High-intensity focused ultrasound treatment of liver tumours: Post-treatment MRI correlates well with intra-operative estimates of treatment volume. Br J Radiol 2012;85: 1363–70.
161. Sherwood V, Civale J, Rivens I, Collins DJ, Leach MO, ter Haar GR. Development of a hybrid magnetic resonance and ultrasound imaging system. Biomed Res Int 2014;2014:914347.
162. Wang Q, Guo R, Rong S, Yang G, Zhu Q, Jiang Y, et al. Noninvasive renal sympathetic denervation by extracorporeal high-intensity focused ultrasound in a pre-clinical canine model. J Am Coll Cardiol 2013;61:2185–92.
163. Choe JW, Nikoozadeh A, Oralkan O, Khuri-Yakub BT. GPU-based real-time volumetric ultrasound image reconstruction for a ring array. IEEE Trans Med Imaging 2013;32:1258–64.
164. Idzenga T, Gaburov E, Vermin W, Menssen J, de Korte C. Fast 2-D ultrasound strain imaging: The benefits of using a GPU. IEEE Trans Ultrason Ferroelectr Freq Control 2014;61:207–13.
165. Sun L, Collins CM, Schiano JL, Smith MB, Smith NB. Adaptive real-time closed-loop temperature control for ultrasound hyperthermia using magnetic resonance thermometry. Concepts Magn Reson Part B Magn Reson Eng 2005;27B:51–63.
166. Salomir R, Rata M, Lafon C, Cotton F, Delemazure AS, Palussiere J, et al. Automatic feedback control of the temperature for MRI-guided therapeutic ultrasound. Conf Proc IEEE Eng Med Biol Soc 2007;2007:222–5. DOI: 10.1109/IEMBS.2007.4352263.
167. Tang K, Choy V, Chopra R, Bronskill MJ. Conformal thermal therapy using planar ultrasound transducers and adaptive closed-loop MR temperature control: demonstration in gel phantoms and ex vivo tissues. Phys Med Biol 2007;52:2905–19.

168. NDjin WA, Burtnyk M, Lipsman N, Bronskill M, Kucharczyk W, Schwartz ML, et al. Active MR-temperature feedback control of dynamic interstitial ultrasound therapy in brain: In vivo experiments and modeling in native and coagulated tissues. Med Phys 2014;41:093301.
169. Owen NR, Chapelon JY, Bouchoux G, Berriet R, Fleury G, Lafon C. Dual-mode transducers for ultrasound imaging and thermal therapy. Ultrasonics 2010;50:216–20.
170. Chapelon JY, Cathignol D, Cain C, Ebbini E, Kluiwstra JU, Sapozhnikov OA, et al. New piezoelectric transducers for therapeutic ultrasound. Ultrasound Med Biol 2000;26: 153–9.
171. Wong SH, Watkins RD, Kupnik M, Pauly KB, Khuri-Yakub BT. Feasibility of MR-temperature mapping of ultrasonic heating from a CMUT. IEEE Trans Ultrason Ferroelectr Freq Control 2008;55: 811–18.
172. Ziadloo A, Vaezy S. Real-time 3D image-guided HIFU therapy. Conf Proc IEEE Eng Med Biol Soc 2008;2008:4459–62.
173. Fukuda H, Numata K, Nozaki A, Morimoto M, Kondo M, Tanaka K, et al. Usefulness of US-CT 3D dual imaging for the planning and monitoring of hepatocellular carcinoma treatment using HIFU. Eur J Radiol 2011;80:e306–10.
174. Bihari P, Shelke A, New TH, Mularczyk M, Nelson K, Schmandra T, et al. Strain measurement of abdominal aortic aneurysm with real-time 3D ultrasound speckle tracking. Eur J Vasc Endovasc Surg 2013;45:315–23.
175. Mauri G, Cova L, De Beni S, Ierace T, Tondolo T, Cerri A, et al. Real-Time US-CT/MRI image fusion for guidance of thermal ablation of liver tumors undetectable with US: Results in 295 Cases. Cardiovasc Intervent Radiol 2014. doi: 10.1007/s00270-014-0897-y.
176. Lorsakul A, Gamarnik V, Duan Q, Russo C, Angelini E, Homma S, et al. Impact of temporal resolution on LV myocardial regional strain assessment with real-time 3D ultrasound. Conf Proc IEEE Eng Med Biol Soc 2012;2012:4075–8.
177. Constanciel E, NDjin WA, Bessiere F, Chavrier F, Grinberg D, Vignot A, et al. Design and evaluation of a transesophageal HIFU probe for ultrasound-guided cardiac ablation: simulation of a HIFU mini-maze procedure and preliminary ex vivo trials. IEEE Trans Ultrason Ferroelectr Freq Control 2013;60: 1868–83.
178. Curiel L, Hynynen K. Localized harmonic motion imaging for focused ultrasound surgery targeting. Ultrasound Med Biol 2011; 37:1230–9.